Monthly Notices
of the
ROYAL ASTRONOMICAL SOCIETY

MNRAS **465,** 68–75 (2017)
Advance Access publication 2016 October 26

doi:10.1093/mnras/stw2742

Flare-production potential associated with different sunspot groups

S. Eren,[1⋆] A. Kilcik,[1⋆] T. Atay,[1] R. Miteva,[2] V. Yurchyshyn,[3,4⋆] J. P. Rozelot[5] and A. Ozguc[6]

[1]*Faculty of Science, Department of Space Science and Technologies, Akdeniz University, 07058 Antalya, Turkey*
[2]*Space Research and Technology Institute, Bulgarian Academy of Sciences, Acad. Georgy Bonchev, 1113 Sofia, Bulgaria*
[3]*Big Bear Solar Observatory, New Jersey Institute of Technology, Big Bear City, CA 92314, USA*
[4]*Korea Astronomy and Space Science Institute, 776 Daedeok-daero, Yuseong-gu, Daejeon 305-348, South Korea*
[5]*Observatoire de la Cote d'Azur , Nice University, Bvd de l'Observatoire, CS 34229, F-06304 Nice Cedex 4, France*
[6]*Kandilli Observatory and Earthquake Research Institute, Bogazici University, 34684 Istanbul, Turkey*

Accepted 2016 October 21. Received 2016 October 21; in original form 2016 March 7

ABSTRACT

In this study, we analysed different types (C, M, and X classes) of X-ray solar flares occurring in sunspot groups. The data cover 1996–2014 time interval, and a total of 4262 active regions (ARs) were included in the data set. We defined the solar-flare-production potential as the ratio of the total number of flares observed in a sunspot group to the total number of the same-class sunspot groups. Our main findings are as follows: (1) large and complex sunspot groups (D+E+F) have the flare-production potential about eight times higher than the small and simple (A+B+C+H) ARs; (2) 79 per cent of all flares were produced by the large and complex sunspot groups, while only 21 per cent of flares were produced by the small groups; (3) the largest and the most complex F-class (very large and very complex) sunspot groups exhibit the highest flare-production potential (2.16 flare per sunspot group), while the smallest and the least complex A class sunspot groups show the lowest (0.05 flare per group) flare-production potential; (4) temporal variation of sunspot counts, sunspot group areas, and the total number of flares (including C flares) showed similar time profiles during both cycles with multiple peaks; (5) the mean area of ARs very well describes the flare-production potential of each group with the regression coefficient of $R^2 = 0.99$. Most of these sunspot groups (>70 per cent) are, according to the Zurich Classification, complex ARs.

Key words: Sun: activity – Sun: atmosphere – Sun: flares – sunspots.

1 INTRODUCTION

Sunspots are strong magnetic-field concentrations in the solar atmosphere. They appear dark in white-light images because of their low temperature, which is due to suppressed convection in the magnetized plasma regions that leads to lower energy flux into a sunspot as compared to their surroundings. Sunspots are transient phenomenon with a lifetime that can vary from a few days to a few weeks or even months. Sunspot data, due to the very long temporal coverage (about 400 years), are valuable for understanding the past variations of solar activity as well the development of modern prediction schemes. They have been systematically observed since the invention of the telescope in 1610 (e.g. Vaquero, Gallego & Trigo 2007) and their counts can also be retrieved from old books extending back in time. Sunspot groups are generally classified according to their morphology and longitudinal extent (LE). They were first separated in five main classes by Cortie (1901), based on their shape and evolution. Later, Waldmeier (1938) introduced the Zurich classification by dividing the sunspot groups in nine classes, which were called A, B, C, D, E, F, G, H, and J. Finally, McIntosh (1990) modified the Zurich classification to better describe the relationship between sunspots and solar flares and to better account for the sunspot main characteristics such as class, size, complexity, etc. The modified Zurich (also called McIntosh) classification now includes seven classes (A, B, C, D, E, F, and H). Note that the G class in Zurich classification was merged into E and F classes, and the J class was merged into the H group. This new classification is based on three main parameters. The first one is the modified Zurich class and it describes the sunspot group morphology and evolution. The second parameter describes the main sunspot in the group according to its penumbral characteristics. The last parameter shows the complexity of the sunspot distribution inside a group.

Complexity of the magnetic fields and the degree of their non-potentiality are responsible for occurrence of solar flares, which are

⋆E-mail: salihaeren@akdeniz.edu.tr (SE); alikilcik@akdeniz.edu.tr (AK); vayur@bbso.njit.edu (VY)

© 2016 The Authors
Published by Oxford University Press on behalf of the Royal Astronomical Society

Downloaded from https://academic.oup.com/mnras/article/465/1/68/2417463 by Akdeniz Universitesi user on 20 September 2021

manifested as sudden increase of chromospheric and coronal (as well as photospheric in the case of strong flares) brightening observed on the solar disc over a wide range of solar spectra (Švestka 1966). Flares are indirectly associated with accelerated high-energy particles, coronal mass ejections (CMEs), and geomagnetic storms. Solar material heated to millions of degrees overcomes the resistance of the solar coronal magnetic fields and escapes into interplanetary space during an eruption. The typical amount of energy released during a solar flare can range between 10^{27} and 10^{32} erg depending on the flare type (e.g. Fletcher et al. 2011). Flares reach their brightness peak in a very short time and then fade gradually away. They affect all the outer layers of the solar atmosphere (photosphere, chromosphere, and corona), as well as the near-space environment and ground-based infrastructures (pipelines and electricity grids, etc.) on the Earth. During these events, electrons, protons, and heavy ions can be accelerated up to speeds close to the speed of light and the magnetic energy is released in all ranges of the electromagnetic spectrum. It is known that faster CMEs are typically associated with more powerful solar flares (Moon et al. 2002; Youssef 2013). If a CME erupts in the Earthward direction it can produce a strong geomagnetic storm, which may have destructive effect on the Earth and near-space environment infrastructure, such as pipelines, electronic systems, GPS and navigation, satellites, etc. In general, strong flare activity mostly occurs in complex sunspot groups.

Using white-light data, Carrington (1859) and Hodgson (1859) independently reported in 1859, first-observed solar flare, which was seen as a short-term brightness increase. After the invention of a spectrohelioscope by Hale (1920), regular Hα observations have begun. Later, Kleczek (1952) introduced a flare index, FI:

$$\mathrm{FI} = it, \tag{1}$$

where i is the flare importance defined as a combination of its brilliance and the flare area measured using Hα data, and t is the flare duration in minutes. There are three main groups of flare brilliance: faint (f), normal (n), and bright (b). The flare area is separated into five groups based on the LE of the flaring region: S (LE $< 2^{\circ}$), 1 ($2^{\circ}.1 \leq$ LE $\leq 5^{\circ}.1$), 2 ($5^{\circ}.2 \leq$ LE $\leq 12^{\circ}.4$), 3 ($12^{\circ}.5 \leq$ LE $\leq 24^{\circ}.7$), and 4 (LE $> 24^{\circ}.7$). Using these two parameters, solar flares can be classified in 15 different classes such as Sf, 1n, 4b, etc.

The X-ray classification of solar flares began in the 1970s with the advent of Earth-orbiting satellites. Solar flares are associated with powerful X-ray radiation, which can be measured and used to describe the intensity of an event. There are currently five X-ray classes of solar flares (A, B, C, M, and X),[1] where each letter corresponds to the power of 10 [−8, −7, −6, −5, and −4, respectively]) of the peak flare flux expressed (in watt per square metre, W m^{-2}) and measured in the 1–8 Å (100–800 pm) spectral range. The X-ray flux from the Sun is regularly monitored by the Geostationary Operational Environmental Satellite and is now commonly used to indicate the peak flux of a flare. The above classes of solar flares can be described in the following way:

(i) A-class flares are the smallest and often called subflares.

(ii) B-class flares are very small in size and their effect on Earth is negligible. They may also be considered as subflares.

(iii) C-class flares are small mostly without plasma eruptions and with few noticeable consequences on Earth.

(iv) M-class flares are medium sized. Many M-class flares are accompanied with a CME. They generally cause brief radio blackouts that affect Earth's polar regions. Minor radiation storms sometimes follow an M-class flare.

(v) X-class flares are large and powerful; they are major cause of radio blackouts and long-lasting radiation storms in the upper Earth's atmosphere.

The A, B, C, and M classes are further subdivided into 10 equidistant subunits, while the X-class is open ended. Each X-ray class is then 10 times stronger than the previous one, with a maximum flux of the order of 10^{-4} W m^{-2}. Hence, the subclasses follow a linear relationship; e.g. an M2 flare is twice as powerful as an M1 flare and four times more powerful than a C5 flare. Sometimes flares exceed the *X9.9* class in intensity, so they are expressed as X10, or X20 as the one observed on 2001 April 2 in National Oceanic Atmospheric Administration (NOAA) active region (AR) 9393.

Kilcik et al. (2011a) analysed modified Zurich classification data by grouping them into two categories, 'Small/Simple' (includes A+B+C+H classes) and 'Large/Complex' (D+E+F classes). The authors found that the number of groups in each category varies differently with time during a solar cycle. They concluded that the sunspot groups in the 'Large/Complex' category better correlate with geomagnetic indices (Ap and Dst) as compared to the International Sunspot Number (ISSN) and the 'Small/Simple' category. The relationship between the area of sunspot groups and the flare-occurrence rate was reported previously (Lou 2000; Zharkov & Zharkova 2006). Sammis, Tang & Zirin (2000) analysed the occurrence rate of large flares by comparing the magnetic classification, sunspot group area (SSGA), and the peak soft X-ray flux. They found that the size of the flare is increasing along with the size of the sunspot group. Later, Lee et al. (2012) separated sunspot groups into 'Large' and 'Small' types according to their areas. To describe the changes observed in SSGAs, they also introduced three subgroups as 'decreasing, steady, and increasing' ARs. They found that the flare-occurrence rate and flaring probability grow with the increasing SSGA (see tables 5 and 6 in their paper). On the other hand, Shibata et al. (2013) investigated superflares produced by sun-like stars with large sunspot areas using Kepler satellite data. They concluded that our Sun can generate a super AR once in 800 years, which may be capable of producing a superflare with energy of one order of magnitude higher than the strongest observed solar flares. Aulanier et al. (2013) analysed the largest solar flares observed in the past using a combined numerical magnetohydrodynamic model and reported that energy of the largest possible flares may exceed the current flare energy levels by about six times.

In this study, we focus on the relationship between the X-ray flare-production potential and the first and third parameters of the modified Zurich classification for the 1996–2014 time intervals, which include Solar Cycle 23 (1996–2008) and the ascending and the maximum phases of Solar Cycle 24. The distinction between small and simple and large and complex sunspot groups introduced in Kilcik et al. (2011a) is considered here in more detail by analysing the solar-flare-production potential defined for each sunspot group, as the ratio of the total number of flares observed in a sunspot group to the total number of the same class sunspot groups. Previous studies on the subject were restricted to a shorter temporal coverage (e.g. Lee et al. 2012) or were only focused on strong flares such as M- and X-class flares (e.g. Hudson, Fletcher & McTiernan 2014). In our study, we used 18-yr-long time-series data and included a wider range of the associated flares. In the next section (Section 2), we shortly describe sunspot classifications, and in Section 3, we present methodology and data analysis. The discussion and conclusions are given in Section 4.

[1] For more details, see http://www.esa.int.

Downloaded from https://academic.oup.com/mnras/article/465/1/68/2417463 by Akdeniz Universitesi user on 20 September 2021

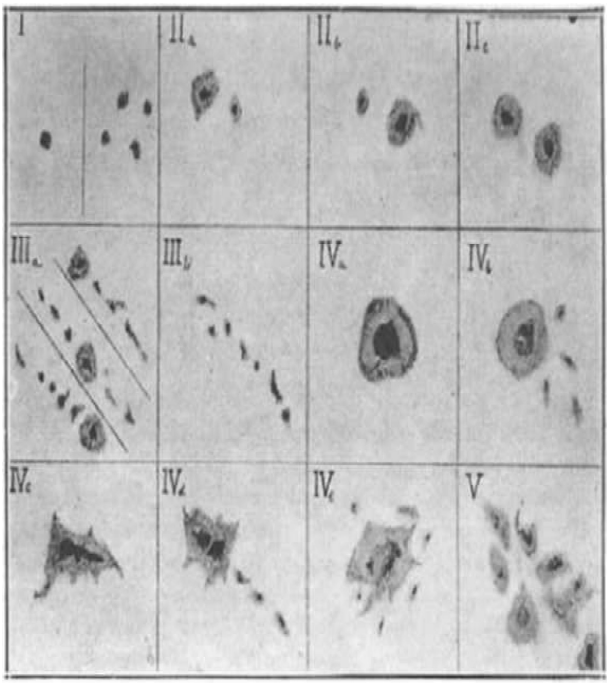


Figure 1. Cortie sunspot group classification. (Source: e.g. Carrasco et al. 2015).

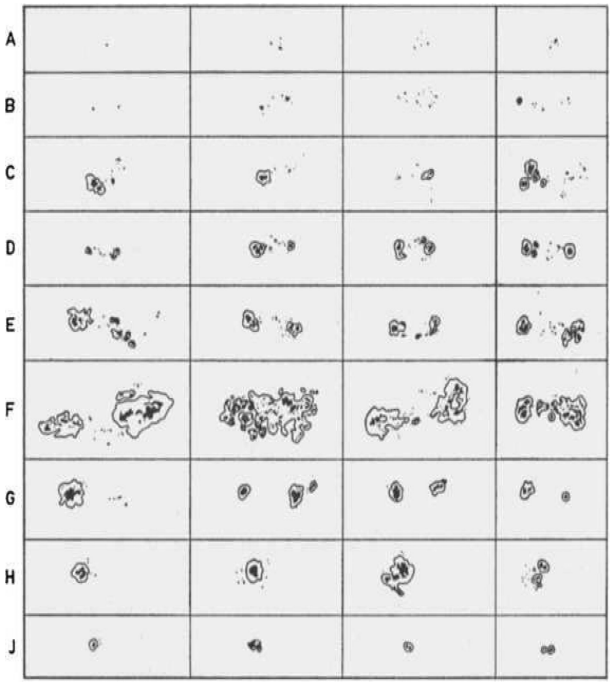


Figure 2. Waldmeier sunspot group classification. (Source: e.g. Carrasco et al. 2015).

2 SUNSPOT CLASSIFICATIONS

2.1 Cortie classification

Cortie (1901) classified the sunspot groups in five different main categories based on their shapes and evolution (see Fig. 1).

(i) Type I: a group of one or scattered spots.
(ii) Type II: the two spot formation –

(a) Type IIa: in which the leader is the principal spot.
(b) Type IIb: in which the following spot is the principal spot.
(c) Type IIc: in which both spots are more or less equal.

(iii) Type III: a train of spots –

(a) Type IIIa: with well-defined principal spots.
(b) Type IIIb: without well-defined principal spots, but consisting mostly of penumbral patches with shattered irregular umbra.

(iv) Type IV: single spots –

(a) Type IVa: a single spot of round and regular outline.
(b) Type IVb: a single spot of round and regular outline with small companions.
(c) Type IVc: a single spot of irregular outline.
(d) Type IVd: a single spot of irregular outline with a train of smaller companions.
(e) Type IVe: a single spot of irregular outline with smaller companions not in a train.

(v) Type V: an irregular group of larger spots.

2.2 Waldmeier (Zurich) classification

Zurich classification was developed (Waldmeier 1938, 1955) according to the polarity configurations, the size and complexity, evolution and morphology, and the presence or absence of penumbra in the sunspot groups. Waldmeier divided sunspot groups in nine different categories (see Fig. 2) depending on the following criteria.

(i) A: a single spot, or a group of spots. There is no penumbra, and no obvious bipolar configuration.
(ii) B: a group of spots without penumbra. The group is dominated by two spots that mark the two magnetic polarities; the bipolar character is clearly noticeable.
(iii) C: bipolar group; one of the principal spots has a penumbra.
(iv) D: bipolar group; both principal spots have a penumbra, but at least one of them still has a simple structure. The group extends over less than 10° on the solar disc.
(v) E: large bipolar group, extending over more than 10° on the Sun. Both principal spots have a penumbra and often a complex structure.
(vi) F: very large and very complex, bipolar group, extending over $\geq$15° on the solar disc.
(vii) G: large bipolar group, of extent $\geq$10°. The small spots in between the principal ones; have disappeared.
(viii) H: unipolar spot with penumbra, diameter (including penumbra) $\geq$2.5.
(ix) J: as H, but diameter $<$2.5.

2.3 McIntosh (modified Zurich) classification

Both Cortie and Zurich classifications show a low correlation with other solar-activity indicators such as sunspot areas, solar flares, etc. It has necessitated the improvement of revising the present classification system as done by McIntosh (1990). This classification is mainly based on three parameters that are used today. The first parameter describes morphology and evolution of a group, the second parameter describes the shape of the biggest spot in the group, and the third parameter describes the distribution of spots inside a sunspot group (see Fig. 3). According to the first parameter of this classification, sunspot groups are divided into seven classes.

Downloaded from https://academic.oup.com/mnras/article/465/1/68/2417463 by Akdeniz Universitesi user on 20 September 2021

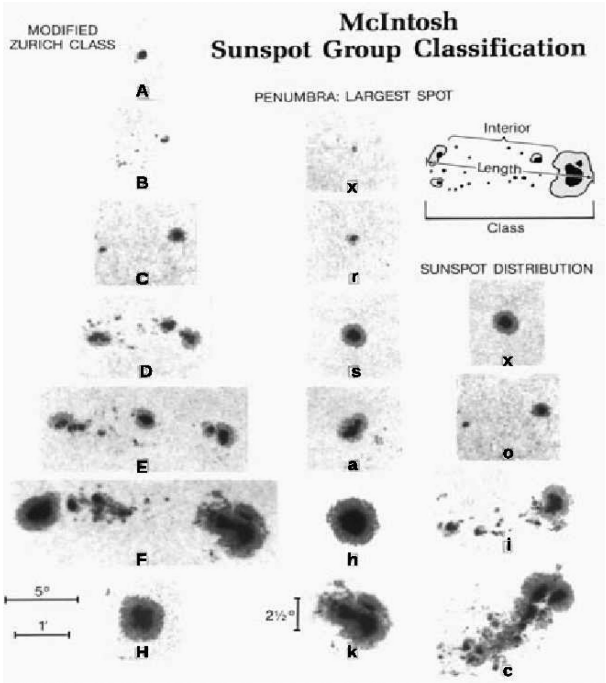


Figure 3. McIntosh sunspot group classification. (Source: McIntosh 1990).

(i) A: unipolar group with no penumbra, representing either the formative or final stage of evolution in a spot group.

(ii) B: bipolar group without penumbra on any spot.

(iii) C: bipolar group with penumbra on one end of the group, in most cases surrounding the largest of the leader umbrae.

(iv) D: bipolar group with penumbra on spots at both ends of the group, and with length $\leq 10^{\circ}$.

(v) E: bipolar group with penumbra on spots at both ends of the group, and with length defined as $10^{\circ} <$ length $\leq 15^{\circ}$.

(vi) F: bipolar group with penumbra on spots at both ends of the group, and length $>15^{\circ}$.

(vii) H: unipolar group with penumbra. The principal spot is usually the leader spot remaining from a pre-existing bipolar group.

According to the second parameter, there are six different groups (x, r, s, a, h, k). They describe the penumbra of largest spot in the group. The third parameter describes the sunspot distribution inside the group and there are four groups (x, o, i, c) according to this parameter.

2.4 Mount Wilson magnetic classification

Classification of the magnetic character of sunspots according to rules set forth by the Mount Wilson Observatory in California is as following.

(i) Alpha: a unipolar sunspot group.

(ii) Beta: a sunspot group having both positive and negative magnetic polarities (bipolar), with a simple and distinct division between the polarities.

(iii) Gamma: a complex AR in which the positive and negative polarities are so irregularly distributed as to prevent classification as a bipolar group.

(iv) Beta–Gamma: a sunspot group that is bipolar but which is sufficiently complex that no single, continuous line can be drawn between spots of opposite polarities.

(v) Delta: a qualifier to magnetic classes indicating that umbrae separated by less than 2 deg within one penumbra have opposite polarity.

(vi) Beta–Delta: a sunspot group of general beta magnetic classification but containing one (or more) delta spot(s).

(vii) Beta–Gamma–Delta: a sunspot group of beta–gamma magnetic classification but containing one (or more) delta spot(s).

(viii) Gamma–Delta: a sunspot group of gamma magnetic classification but containing one (or more) delta spot(s).

More than half of the observed sunspot groups are Alpha and Beta classes. Bigger sunspot groups mostly display Beta–Gamma or Beta–Gamma–Delta configuration, which are generally more complex.[2]

3 DATA, ANALYSIS, AND RESULTS

The sunspot-classification data used in this study were taken from the Solar Monitor web site.[3] The raw data set consisted of a total of 30 939 sunspot group measurements which cover the 1996–2014 time intervals. They include the NOAA identification numbers, SSGAs, sunspot counts (SSCs), modified Zurich classes of sunspots, X-ray flare, etc.

Fig. 4 shows temporal variations of different X-ray-class flares. We encountered that all flare classes display double peaks: the C-class flares have almost the same magnitude double peaks in 2000 April and again in 2002 June, the M-class flares peaked in 2000 April and 2001 August and the second peak is more prominent than the first one, and the X-class flares have also almost the same intensity peaks in 2000 November and in 2003 August during Solar Cycle 23. Note that the second peak was much wider than the first one. On the contrary, all class flares behave similarly during the current Solar Cycle 24: the first maximum is observed near 2012 January, and the second maximum occurred near 2014 April. Note that although the average number of M- and X-class flares is much lower during Solar Cycle 24 as compared to Cycle 23, the number of C-class flares is almost the same and they are the most abundant flares compared to others (M- and X-class flares). It is expected that the C-class trend dominates the characteristics of all flares, so that the total number of flares in both cycles remains nearly the same.

Fig. 5 shows the monthly mean SSCs, SSGAs, and the number of X-ray flares during the investigated time period. A very good agreement exists between all data sets for both cycles. All the data sets exhibit double or multiple peak features. There appear to be some strong peaks in the X-ray-flare profile during the descending phase of Solar Cycle 23. It is interesting to note that the corresponding features also appear clearly in the SSGA. In addition to this, the X-ray-flare number is at nearly the same level in both cycles, so it depends on the C-class solar-flare number.

In Fig. 6, we present the percentage of observed flare number in each group (left-hand panel) and the flare-production potential (right-hand panel). The F-class sunspot groups (the largest and the most complex) display the highest flare-production potential (2.16 flare/sunspot group), while the class A sunspot groups (the smallest and the least complex) have the lowest (0.05 flare/sunspot group). In general, the large and complex sunspot groups (D+E+F) display the flare-production potential eight times higher than the small and simple groups (A+B+C+H). One-third (33 per cent) of all flares were produced by the D-class sunspot groups, while only about

[2] www.spaceweatherlive.com
[3] www.solarmonitor.org

Downloaded from https://academic.oup.com/mnras/article/465/1/68/2417463 by Akdeniz Universitesi user on 20 September 2021

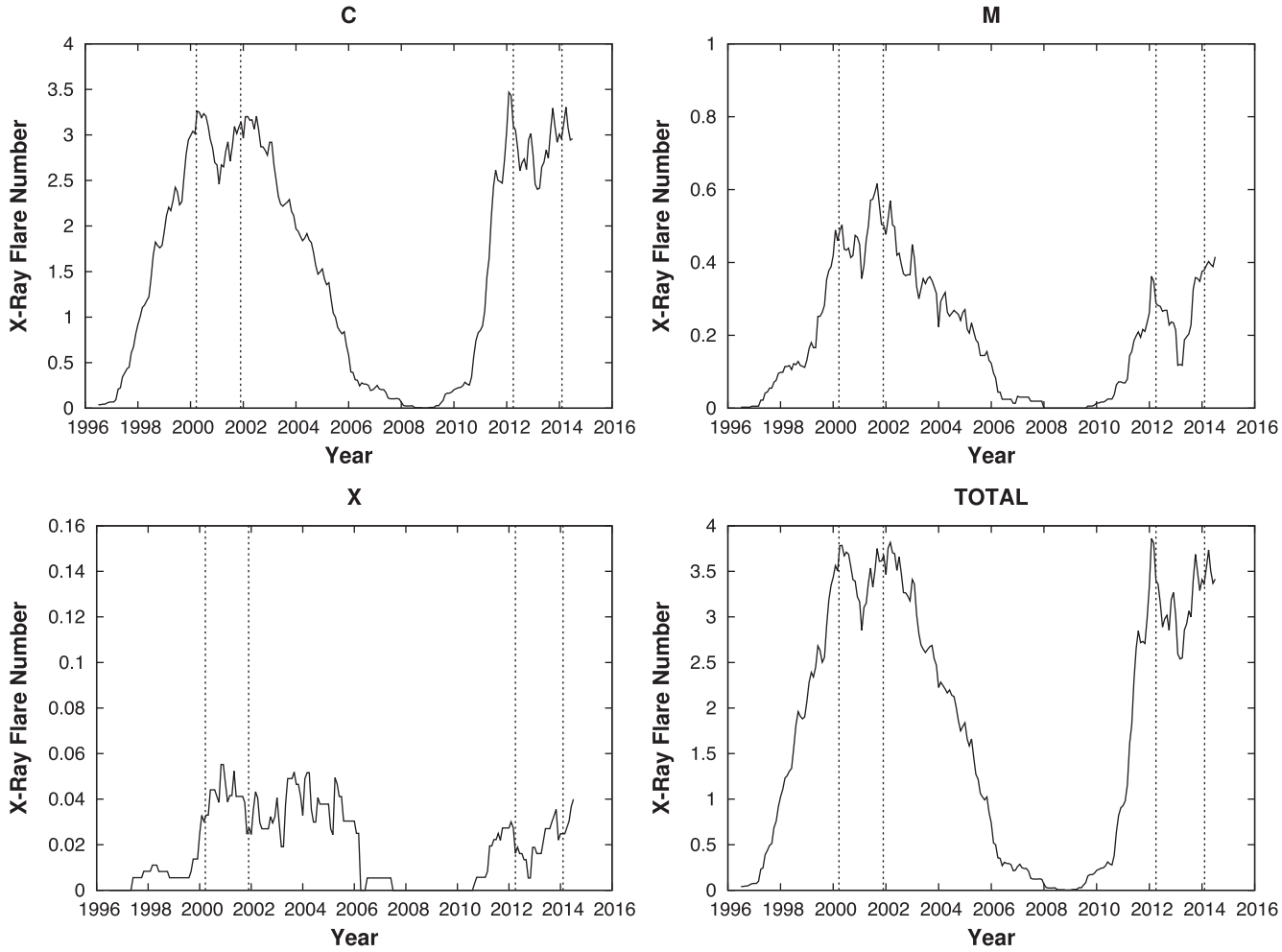


Figure 4. Temporal variations of the daily total number of flares averaged over a month for different flare classes (C, M, X, and C+M+X), respectively. All data are smoothed with a 12-step running average filter. Vertical dotted lines indicate the first and the second maxima of the ISSN.

1 per cent of all flares were produced by the A-class groups. In general, 79 per cent of all flares were produced by the large and complex sunspot groups, while only 21 per cent of them were associated with small and simple ARs. It is clearly seen that the flare-production potential of sunspot groups from A to F show an exponential variation (see Fig. 6, right-hand panel).

We list some statistical results for each McIntosh class used in this study in Table 1. Here we emphasize that the D class has the maximum number of sunspot groups (7283) while the F class has the minimum (1011). As shown in Table 1, the total number of D-class sunspot groups are about seven times that of the F groups. While the flare-production potential of the F-class sunspot groups is about four times higher than that of the D class.

Fig. 7 shows the mean area of sunspot groups in millionths of solar hemisphere (MSH) for each of the modified Zurich classes (see Fig. 3). As seen from this figure, the mean area of sunspot groups is increasing exponentially with the sunspot group class (from A to F), *which is* similar to the flare-production-potential variation (see Fig. 6, right-hand panel). In Fig. 8, we plot the mean area versus flare-production potential of each sunspot group. The two parameters are strongly correlated ($R^2 = 0.993$, $t = 24.92$, df $= 5$, $p < 0.001$). Here, R^2 is the regression coefficient, t is the table value of the Student t-test, df is the degrees of freedom, and p is the significance level of the test. The above data allowed us to argue that the size of the sunspot groups is directly related to its flare-production potential, so that the larger ARs have higher potential to produce numerous solar flares. Note that such a strong linear relationship between the SSGA and the flare-production potential has not been reported before in the literature.

We also investigated the relationship between the SSGA and complexity parameter represented by the third parameter, c, in the McIntosh classification schema. As shown in Table 2, complex groups on average have larger area than non-complex ones. This is true for both large and small ARs.

4 CONCLUSIONS AND DISCUSSION

In this study, we analysed the flare-production potential defined as the ratio of the total number of flares observed in a sunspot group to the total number of the same-class sunspot groups and we report the following.

(1) Large and complex sunspot groups (D+E+F) have the flare-production potential about eight times higher than the small and simple (A+B+C+H) ARs.

(2) 79 per cent of all flares were produced by the large and complex sunspot groups, while only 21 per cent of them were produced by small ARs.

Downloaded from https://academic.oup.com/mnras/article/465/1/68/2417463 by Akdeniz Universitesi user on 20 September 2021

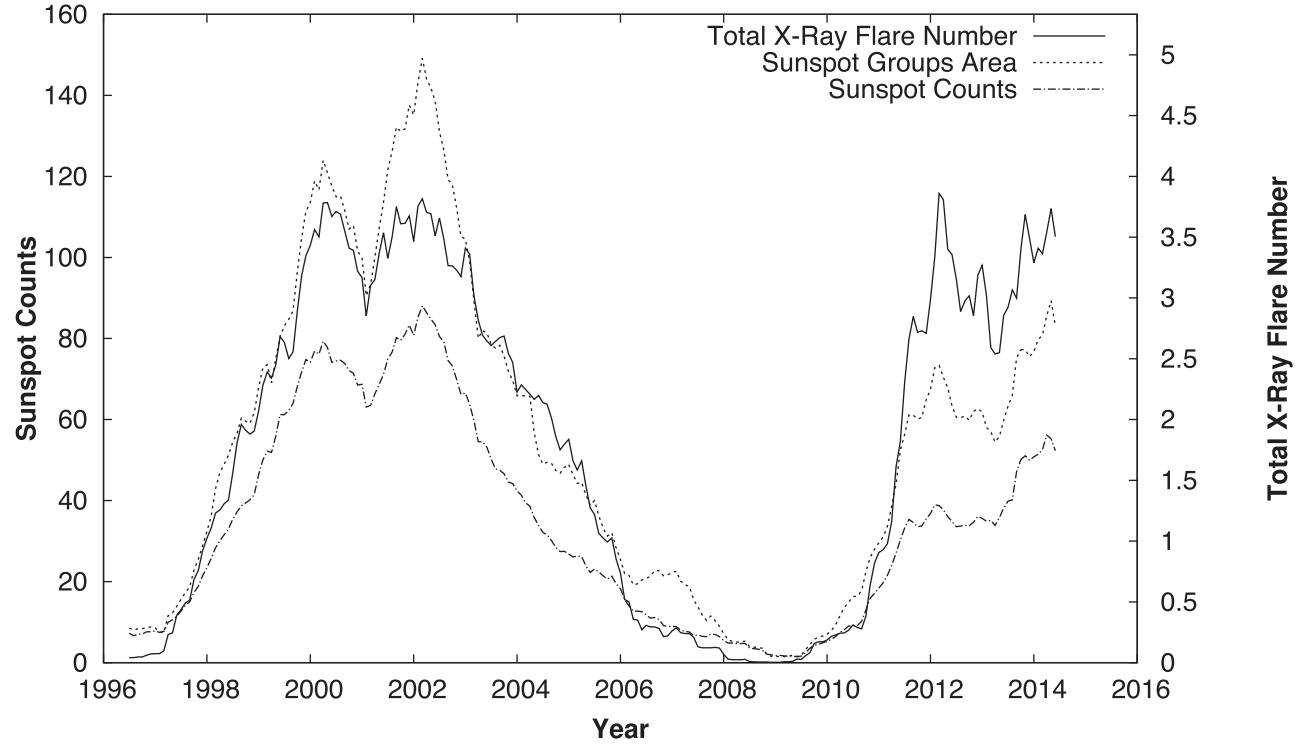


Figure 5. Temporal variations of the daily total SSC, SSGA, and the number of X-ray flares averaged over a month. All data were smoothed with a 12-step running average filter. For display purposes, the SSGAs data were divided by 100.

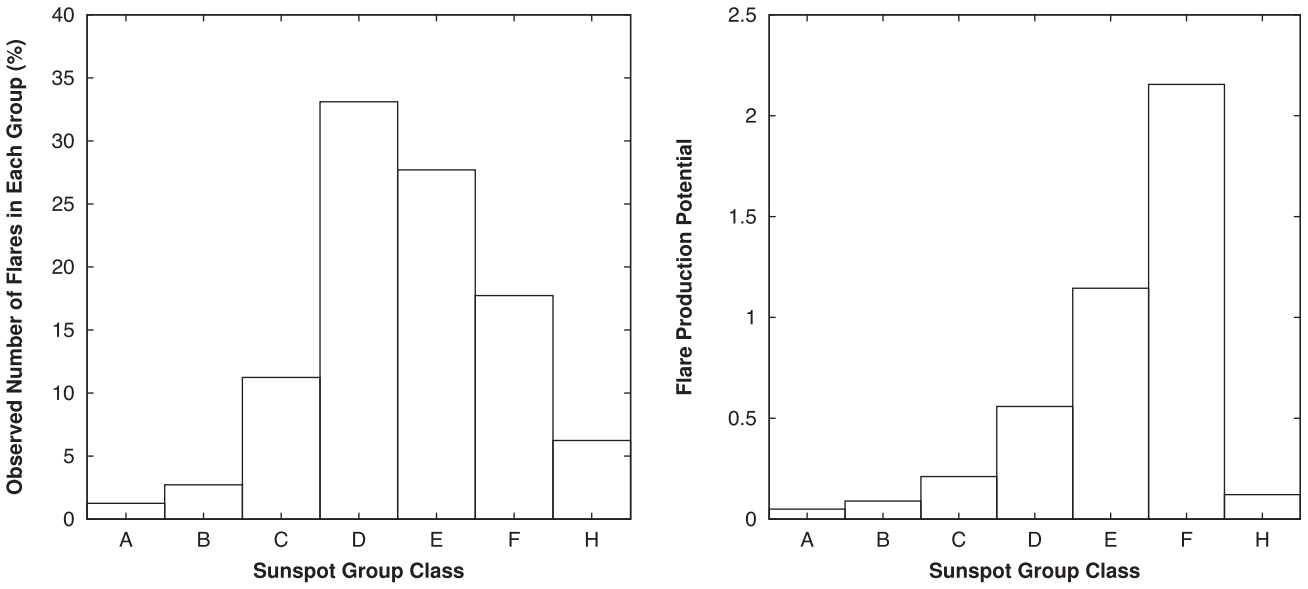


Figure 6. Distribution of the observed number of flares depending on the Zurich class of the sunspot groups (left-hand panel) and flare-production potential of these groups (right-hand panel).

(3) The largest and the most complex F-class sunspot groups display the highest flare-production potential (2.16 flare/sunspot group), while the A-class sunspot groups (the smallest and the least complex) have the lowest flare-production potential (0.05 flare/sunspot group).

(4) Temporal variation of SSCs, SSGAs, and the total number of flares (including C flares) showed similar time profiles during both cycles with multiple peaks.

(5) The mean area of sunspot groups very well describes ($R^2 = 0.993$, $t = 24.92$, df $= 5$, $p < 0.001$) the flare-production potential of each group during the investigated time period (1996–2014). There is a general link between the AR area and the degree of complexity of associated magnetic fields.

The relationship between the flare-occurrence rate and the sunspot number/area has been previously *studied* by a number of

Downloaded from https://academic.oup.com/mnras/article/465/1/68/2417463 by Akdeniz Universitesi user on 20 September 2021

Table 1. For each of the McIntosh sunspot groups A to H is given: the total number of sunspot groups and flares, the number of flares calculated separately for each class of sunspot groups, the flare-production potential of these groups and the total number of each flare/each group.

Sunspot groups	Total number of sunspot groups	Total number of flares	Observed flare number for each class of sunspot groups (per cent)	Flare-production potential per group
A	3083	154	1.25	0.05
B	3731	335	2.73	0.09
C	6545	1381	11.24	0.21
D	7283	4069	33.11	0.56
E	2975	3405	27.71	1.15
F	1011	2179	17.73	2.16
H	6311	767	6.24	0.12

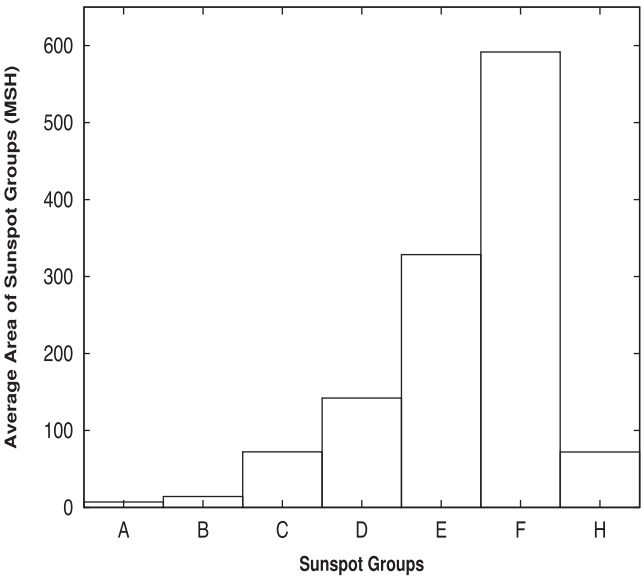


Figure 7. Distribution of SSGA in millionths of solar hemisphere (MSH) for each modified Zurich sunspot group.

authors (e.g. Lou 2000; Sammis et al. 2000; Zharkov & Zharkova 2006; Lee et al. 2012, and references therein). These studies were either based on shorter time intervals or limited selection of sunspot classes and flare intensity. Here, we analysed all classes of sunspot groups (A, B, C, D, E, F, and H) in more detail and calculated their flare-production potential and the percentage of X-ray-flare numbers produced by individual sunspot groups, separately. We found that the solar-flare-production potential and the mean SSGAs are nearly identical during the investigated time interval (see Fig. 8). This analysis not only confirms previous reports but also suggests that the Zurich complexity parameter can be used for a mid-term prognosis of flaring activity.

About 80 per cent of all flares were produced by only three sunspot group classes (D, E, and F). Earlier, Kilcik et al. (2011b) reported that the number of large and complex groups (D, E, and F classes) better correlates with solar and geomagnetic activity than the ISSN and/or the small and simple groups (A, B, C, and H classes). These two reports indicate that the majority of geo-effective events originate in D-, E-, and F-class ARs. Moreover, both the number of large ARs (Kilcik et al. 2011a) and the number

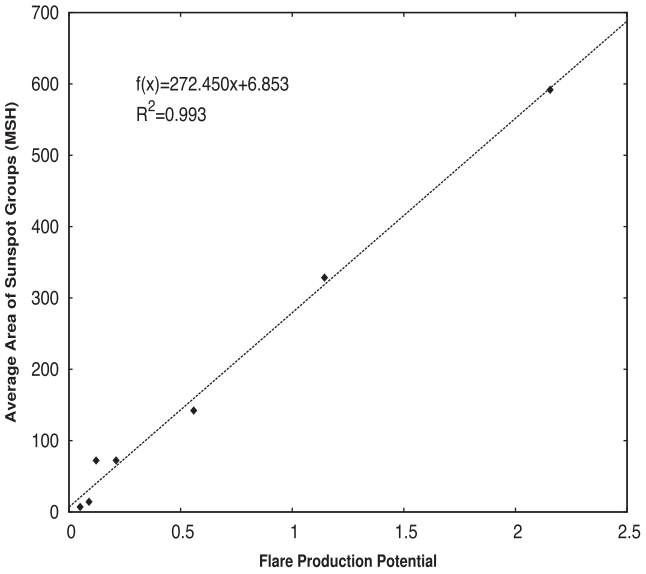


Figure 8. The relationship between the mean sunspot area (MSH) and the flare-production potential.

Table 2. The mean sunspot area listed separately for small and simple and large and complex sunspot groups. The area is measured in millionth of solar hemisphere.

		Mean sunspot areas
Small/simple	Complex	180.00 (75 per cent)
	Non-complex	41.40 (25 per cent)
Large/complex	Complex	604.56 (69 per cent)
	Non-complex	269.39 (31 per cent)

of M- and X-class solar flares have decreased significantly during the current solar cycle, which further illustrates that the occurrence of M- and X-class flares is mostly limited to the large and complex ARs. Based on long and comprehensive time series, we also find that these ARs constitute about 70 per cent of all flaring ARs. A strong shear along the neutral line is an important factor in producing flares (Schrijver 2016). Large shear is generally achieved in complex and large sunspot groups with extended and curved neutral lines.

Recently, Hudson et al. (2014) analysed the solar-flare productivity of individual ARs during the last four solar cycles. Their analysis only included the distribution of flare productivity of the most productive ARs. They concluded that the size of ARs were not of particular importance for the flare production, while the area of magnetic complexity is more important. Aulanier et al. (2013) reported that flares are developing over about 30 per cent of the area of an AR, which is at the same time the area where the most complex magnetic structures are concentrated. Thus the data suggest that the connection reported here between the AR size and the flare-production potential in fact reflects the connection between the complexity area and the flaring potential. Aulanier et al. (2013) and Shibata et al. (2013) present further theoretical evidence for the connection between complexity area and flare production. While Shibata et al. (2013) argue for a super AR with a total magnetic flux of 10^{23} Mx, which is one order of magnitude higher than a typical large solar AR, capable of producing a superflare with energy of about 10^{34} erg; Aulanier et al. (2013) argue that although larger ARs are likely to emerge, the associated flares are not expected to exceed

Downloaded from https://academic.oup.com/mnras/article/465/1/68/2417463 by Akdeniz Universitesi user on 20 September 2021

by much (less than an order of magnitude) the strongest observed solar flare 10^{32} erg.

ACKNOWLEDGEMENTS

The data used in this study were taken from the Solar Monitor web page (http://www.solarmonitor.org/data/). This work, which is a part of the MS thesis of SE, was supported by the Scientific and Technical Council of Turkey (TUBITAK) by the Project 115F031. VY acknowledges support from NSF AGS-1146896, AFOSR FA9550-15-1-0322, and Korea Astronomy and Space Science Institute grants. JPR and VY acknowledge support from the International Space Science Institute (ISSI) in Bern (CH).

REFERENCES

Aulanier G., Démoulin P., Schrijver C. J., Janvier M., Pariat E., Schmieder B., 2013, A&A, 549, 7
Carrasco V. M. S., Lefèvre L., Vaquero J. M., Gallego M. C., 2015, Sol. Phys., 290, 1445
Carrington R. C., 1859, MNRAS, 20, 13
Cortie A. L., 1901, ApJ, 13, 260
Fletcher L. et al., 2011, in Johns-Krull C. M., Browning M. K., West A. A., eds, ASP Conf. Ser. Vol. 448, 16th Cambridge Workshop on Cool Stars, Stellar Systems, and the Sun. Astron. Soc. Pac., San Francisco, p. 441
Hale G. E., 1920, Nature, 105, 266
Hodgson R., 1859, MNRAS, 20, 15
Hudson H., Fletcher L., McTiernan J., 2014, Sol. Phys., 289, 1341
Kilcik A., Yurchyshyn V. B., Abramenko V., Goode P. R., Gopalswamy N., Ozguc A., Rozelot J. P., 2011a, A&A, 727, 6
Kilcik A., Yurchyshyn V. B., Abramenko V., Goode P. R., Ozguc A., Rozelot J. P., Cao W., 2011b, A&A, 731, 8
Kleczek J., 1952, Publ. Cent. Inst. Astron, No. 22, Prague
Lee K., Moon Y.-J., Lee J.-Y., Lee K.-S., Na H., 2012, Sol. Phys., 281, 639
Lou Y.-Q., 2000, ApJ, 540, 1102
McIntosh P. S., 1990, Sol. Phys., 125, 251
Moon Y.-J., Choe G. S., Wang H., Park Y. D., Gopalswamy N., Yang G., Yashiro S., 2002, ApJ, 581, 694
Sammis I., Tang F., Zirin H., 2000, ApJ, 540, 583
Schrijver C. J., 2016, ApJ, 820, 130
Shibata K. et al., 2013, PASJ, 65, 49
Švestka Z., 1966, Space Sci. Rev., 5, 388
Vaquero J. M., Gallego M. C., Trigo R. M., 2007, Adv. Space Res., 40, 1895
Waldmeier M., 1938, Z. Astrophys., 16, 276
Waldmeier M., 1955, Z. Astrophys., 38, 125
Youssef M., 2013, Earth Moon Planets, 110, 185
Zharkov S. I., Zharkova V. V., 2006, Adv. Space Res., 38, 868

This paper has been typeset from a TEX/LATEX file prepared by the author.

Downloaded from https://academic.oup.com/mnras/article/465/1/68/2417463 by Akdeniz Universitesi user on 20 September 2021